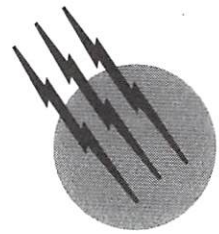

Nanosized Inorganic Clusters

Leroy Cronin
Achim Müller
University of Bielefeld, Germany

Dieter Fenske
University of Karlsruhe, Germany

GLOSSARY

Cluster Group of atoms bound together.
Colloid Particle small enough to remain suspended in solution or gas.
Icosahedron A polyhedron having 20 faces and 12 vertices.
Ligand Molecule bound to a metal atom or cluster.
Nucleation The condensation or aggregation process by which crystals are formed on a minute amount of substance that acts as a nucleus for subsequent crystalline growth.

NANOSIZED CLUSTERS or "nanoclusters" is a term given to particles of any kind of matter, the size of which is greater than that of typical molecules, but is too small to exhibit characteristic bulk properties. Examples of such materials include the family of carbon-based fullerenes, weakly bound van der Waals clusters observed in the gas phase, metal carbonyl clusters, boron carbides and hydrides, metal clusters surrounded by protecting ligands, and metal ions connected by bridging ligands. Of special relevance in this article are those clusters that are sufficiently well-defined and large enough to be at the borderline between the molecule and the bulk. It is in this area that materials with extremely interesting properties have begun to have a profound influence on basic science as well as technology from catalysis to electronically interesting materials. Such materials become even more interesting when they are themselves, as building blocks, organized into a bulk material in a predesigned, desired manner. It is the fabrication of inorganic nanoclusters that lies at the cutting edge of nanodesign and technology today and promises many exciting discoveries and applications tomorrow. We refer here to three important classes of molecular clusters which have been thoroughly characterized and can be seen to be entering the size regime of mesoscopic materials.

I. FROM CLUSTERS TO THE BOUNDARY OF THE METALLIC STATE

Giant metal-based clusters serve as a bridge between molecular clusters and bulk metals. This has implications

Encyclopedia of Physical Science and Technology, Third Edition, Volume 10

for the development of electronic materials, new catalysts and, from an academic point of view, can be used to examine the transition from clusters to the boundary of the metallic state. To examine clusters that lie on the relevant borderline it is important to synthesize systems that do not interact with each other and undergo coalescence, destroying the individuality of the cluster.

To synthesize giant metal-based clusters a preparative approach has to be taken that can yield the metal atoms in their preferable zero-valent oxidation states. Generally, the preparation of these clusters requires the precursor complexes to be dissolved in solution followed by the reduction of the metal ions to a zero-valent state. Once the reduction has occurred—the reduction step can be achieved by metals such as sodium and substrates such as hydrazine, sodium tetrahydroborate, carbon monoxide, and hydrogen—the lifetime of the metal atoms in solution is very short and they tend to coalesce quickly into larger arrangements. The decisive step during the synthetic procedure of clusters of a distinct size, and also with colloids, is to stop the metal-metal aggregation/growth process at the right moment to prevent the formation of a bulk metal. In the gold, platinum, and palladium species this growth can be limited by introducing stabilizing π-acceptor-type ligands, such as phosphines, phenanthroline, and bipyridyl. The role of such ligands is vital in the synthesis of discrete clusters as these ligands act as protecting groups preventing the coalescence of the clusters to form a bulk material.

One example of a material that can be prepared in this manner is given by the gold cluster $Au_{55}(PPh_3)_{12}Cl_6$ which is a two-shell cluster consisting of a central atom that is embedded by two close packed shells of 12 and 42 atoms and is terminated with the protective ligand sheath of twelve triphenylphosphine ligands. The synthesis of this Au_{55} cluster has been improved further by the introduction of a thiol-terminated dendrimer which removes the phosphine ligands and acts as a matrix. The synthesis of other clusters using this approach has shown that the number of metal atoms in the core can follow a set of "magic-numbers," see Fig. 1. Such numbers were postulated since metal skeletons of large molecular clusters could be similar in their structures to small metal crystallites formed on the basis of close-packed (face-center) cubic or hexagonally close-packed arrangements of metal atoms. In the case of the 12-vertex polyhedra, a metal skeleton in the shape of a cuboctahedron or anticuboctahedron was expected as derived from these packing arrangements. The magic numbers can be derived from the formula:

$$N = \frac{1}{3}(10m^3 + 15m^2 + 11m + 3)$$

(N is the magic number and m is the number of shells of the metal atoms packed around the central metal atom in the symmetry of a cuboctahedron or anticuboctahedron). A range of clusters has been synthesized which correspond to magic numbers, for instance M_{13} (one-shell) = $[Au_{13}(diphos)_6](NO_3)_4$, M_{55} (two-shell) = $Au_{55}(PPh_3)_{12}Cl_6$, M_{309} (four-shell) = $Pt_{309}Phen_{36}O_{30\pm10}$ and M_{561} (five-shell) = $Pd_{561}Phen_{60}(OAc_{180})$—the largest cluster to be synthesized and separated preparatively. The five-shell cluster, $Pd_{561}Phen_{60}(OAc_{180})$, results if an acetic acid solution of palladium(II) acetate is reduced by gaseous hydrogen in the presence of small amounts of phenanthroline (phen) followed by the controlled addition of oxygen. In this synthesis the Pd_{561} is the smallest of three different cluster species formed which are 3.60, 3.15, and 2.20 nm in diameter, respectively (without the ligand shell). The electron microscopic study of these particles proves that the different particles are characterized by a distinct number of atomic planes: the 3.60-nm cluster consists of 17 planes, the 3.15-nm cluster of 15 planes, and the 2.20-nm particles of 11 planes. These numbers are compatible with the existence of the magic numbers for each of these cluster types, as described above. In principle, the nth shell consists of $10n^2 + 2$ atoms. Following this model

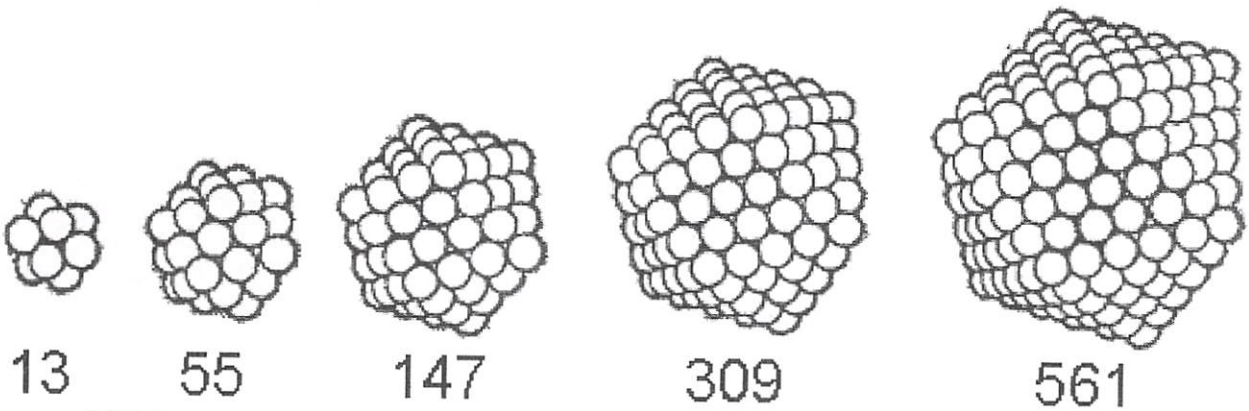

FIGURE 1 A representation of the magic numbers of clusters obtained by surrounding a given atom by successive shells of atoms (the figure shows the cuboctahedral polyhedra formed by the atoms).

the 17 planes in the 3.60-nm clusters are formed by 2057 atoms 15 planes by 1415 atoms and the 11 planes by 561 atoms. Overall, these numbers correspond, for example, to the eight-, seven-, and five-shell clusters with formulas equating to: $Pd_{2057}Phen_{84}O_{1600}$, $Pd_{1415}Phen_{60}O_{1100}$, and $Pd_{561}Phen_{36}O_{200}$, respectively.

Naturally electron microscopy cannot determine the exact number of metal atoms. However, considering the observation that more than 90% of the particles detected with the electron microscope occur with one of the discussed number of planes, it would appear that the natural packing distribution of these assemblies tends toward the description given by the magic numbers. However, in cases where the number of metal atoms in the cluster approaches several hundreds, a set of imperfect clusters/colloids are formed with a certain distribution with respect to size and chemical composition.

The use of colloidal dispersions in the synthesis of metal-based clusters has also afforded routes to ligand-stabilized bimetallic clusters that offer other opportunities to tune the properties of the overall cluster formed. The aim of such work in the future lies in both stabilizing and geometrically linking such cluster entities into 2-D and 3-D networks. If such work was to succeed then new types of storage devices and electronic components of "minute dimensions" may become accessible that probably will never be reached by established methods such as nanolithography.

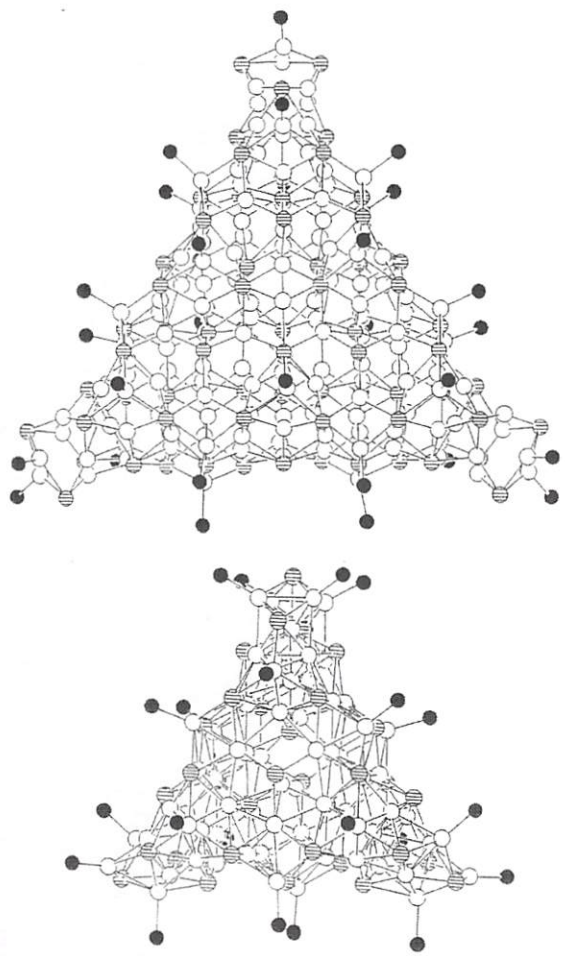

FIGURE 2 Structure of $[Cu_{70}Se_{35}(PEt_3)_{22}]$ and $[Cu_{146}Se_{73}(PPh_3)_{30}]$ (without Et and Ph groups). The Cu atoms are shown as empty spheres, the Se atoms are shown as hatched spheres, and the P as black spheres.

II. FROM CLUSTERS TO SEGMENTS OF SOLID-STATE STRUCTURES

An alternative class of metal clusters which may also provide routes to interesting systems of scientific and technological relevance are derived from metal chalcogenides. During the last few years interest in this class of compounds has increased dramatically, as they can be used as precursors in the production of semiconducting metal selenides and tellurides. A considerable number of multinuclear metal selenide cluster complexes are known now which are protected by a ligand shell thus avoiding further reaction to stable binary selenides. Examples include $[Ni_{34}Se_{22}(PPh_3)_{10}]$, $[Cu_{70}Se_{35}(PEt_3)_{22}]$, and $[Cu_{146}Se_{73}(PPh_3)_{30}]$. These compounds are formed by the reaction of PR_3 complexes (R = organic group) of metal halides with $Se(SiMe_3)_2$, Scheme 1.

The mechanism for cluster formation, and thus the molecular structure of the products, is strongly influenced by the special reaction conditions (temperature, type of copper salt used, type and size of the PR_3 ligand). As expected very often the thermodynamically stable metal chalcogenides are formed, however, calculations have shown that the PR_3-stabilized cluster complexes are metastable.

It is possible to obtain copper chalcogenide clusters which can be approximately described as a section of the structure of the binary Cu_2E phase (E = S, Se, Te) surrounded by PR_3 ligands. Though spherical cluster cores with up to 62 copper atoms do not permit a direct comparison with the binary copper chalcogenides, with increasing cluster size, a tendency toward a layered Cu_2E-type skeleton can be seen. Fragments of the structure of the binary Cu_2Se phase can be recognized for the clusters $[Cu_{70}Se_{35}(PEt_3)_{22}]$ and $[Cu_{146}Se_{73}(PPh_3)_{30}]$ (Fig. 2). In particular, the relation to the Cu_2Se structure can be seen by comparing the Se sublattices of the two cluster compounds. In both clusters a layered segment is formed by the Se ligands, consisting of layers with 10, 15, and 10 Se ($\{Cu_{70}\}$) and 21, 31, and 21 Se atoms ($\{Cu_{146}\}$ cluster), respectively (Fig. 3). Most of the Cu atoms are positioned in the tetrahedral surroundings spanned by the Se atoms.

$$CuX + PR_2R' \xrightarrow[-SiMe_3X]{\begin{array}{l}1.\ \text{organic solvent}\\ 2.\ +E(SiMe_3)_2\end{array}} [Cu_{2n}E_n(PR_2R')_m] \qquad \begin{array}{ll} X & = Cl, OAc \\ R, R' & = \text{org. group} \\ E & = S, Se \end{array}$$

SCHEME 1 General route to the preparaton of metal chalcogenides.

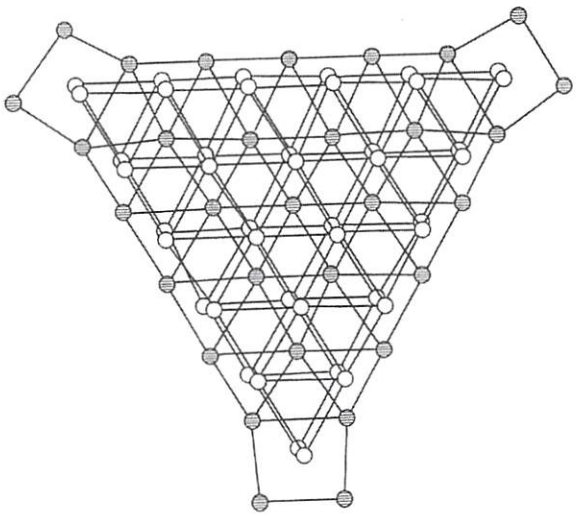

FIGURE 3 Structure of the Se network in $[Cu_{146}Se_{73}(PPh_3)_{30}]$. The Se atoms on the first and third layers are shown as empty spheres and those of the middle layer as hatched spheres.

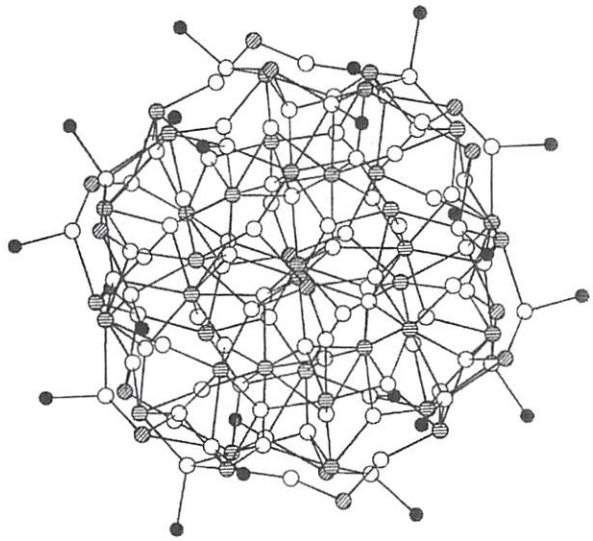

FIGURE 4 Structure of $[Ag_{90}Se_{38}(Se^tBu)_{14}(PEt_3)_{22}]$ without C atoms. Ag atoms are shown as empty spheres, Se atoms are depicted as horizontally hatched spheres, and the Se atoms of the Se^tBu groups are hatched spheres.

The reaction of AgCl, for example, with $Se(SiMe_3)_2$ in the presence of PR_3 usually affords insoluble Ag_2Se, while the corresponding reaction with $R'TeSiMe_3$ preferably provides silver clusters with Te^{2-} and TeR^- ligands. The structures of the compounds formed depend very much upon the type of the tertiary phosphane used and also on the organic group R′. Examples of related compounds with known structures are $[Ag_6(\mu_3\text{-}Te^nBu)_4(\mu\text{-}Te^nBu)_2(PEt_3)_4]$, $[Ag_{10}(TePh)_{10}(PMe_3)_2]_\infty$, $[Ag_{30}(TePh)_{12}Te_9(PEt_3)_{12}]$, $[Ag_{32}(\mu_3\text{-}Te^nBu)_{18}Te_7(PEt_3)_6]$, $[Ag_{46}(TeMes)_{12}Te_{17}(PEt_3)_{16}]$, and $[Ag_{48}(\mu_3\text{-}Te^nBu)_{24}Te_{12}(PEt_3)_{14}]$. Other Ag clusters can be isolated from the reaction of silver carboxylates with $RSeSiMe_3$ (R = organic group) and PR_3 or bidentate phosphanes. The reaction of P^nPr_3 with $^tBuSeSiMe_3$ and silver benzoate in pentane at −40°C affords $[Ag_{30}Se_8(Se^tBu)_{14}(P^nPr_3)_8]$ (Scheme 2). Using the same reaction conditions with PEt_3 as ligands, only the formation of $[Ag_{90}Se_{38}(Se^tBu)_{14}(PEt_3)_{22}]$ can be observed.

However, the $\{Ag_{90}\}$ cluster (Fig. 4) shows no similarity with the corresponding binary phase Ag_2Se but exciting structural details: The Se atoms form a torus-shaped polyhedron, which is built up from Se_3 faces (Fig. 5). The reaction of $Ag(C_{11}H_{23}CO_2)$ with $^nBuSeSiMe_3$ and P^tBu_3 yields $[Ag_{114}Se_{34}(Se^nBu)_{46}(P^tBu_3)_{14}]$ (Fig. 6). If the monodentate phosphane ligands are replaced by bis(diphenylphosphino) propane (dppp), under the same reaction conditions (Scheme 3) (−30°C) the largest known Ag cluster $[Ag_{172}Se_{40}(Se^nBu)_{92}(dppp)_4]$ is formed (Fig. 7).

The layer clusters of the type $\{Ag_{114}\}$ and $\{Ag_{172}\}$ are structurally different from the aforementioned systems, for instance, from the spherical $\{Ag_{30}\}$ and $\{Ag_{90}\}$ clusters. There is a remarkable agreement between the Se skeletons in the $\{Ag_{114}\}$ and $\{Ag_{172}\}$ clusters and that of Ag_2Se (Fig. 8). The cluster structures can realistically be described as sections of the binary phase Ag_2Se. With increasing cluster size, the distribution of the Ag atoms in the molecular structure becomes more random. Obviously there is a tendency to a kind of disordering of the Ag atoms which is also observed in the bulk material Ag_2Se.

$$\left[Ag_{90}Se_{38}(Se^tBu)_{14}(PEt_3)_{22}\right] \xleftarrow[PEt_3]{^tBuSeSiMe_3} Ag(C_6H_5CO_2) \xrightarrow[P^nPr_3]{^tBuSeSiMe_3} \left[Ag_{30}Se_8(Se^tBu)_{14}\left(P^nPr_3\right)_8\right]$$

SCHEME 2 Synthetic route to Ag_{90} and Ag_{30} clusters.

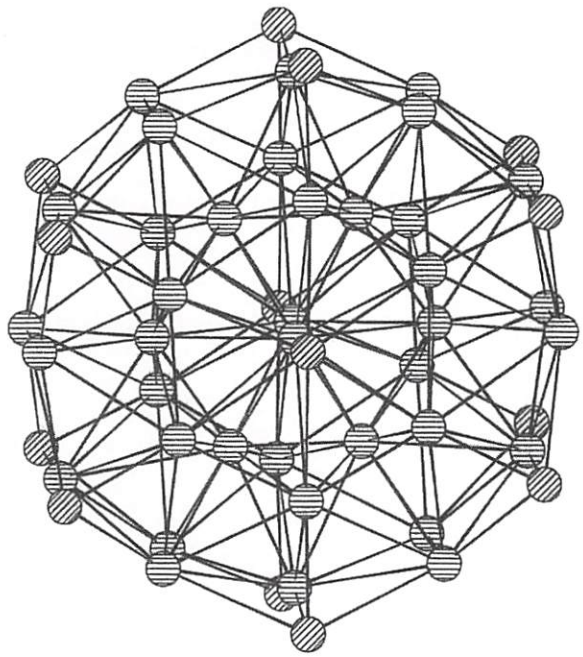

FIGURE 5 Se skeleton in $[Ag_{90}Se_{38}(Se^tBu)_{14}(PEt_3)_{22}]$. Se atoms are shown by the horizontally hatched spheres and the Se atoms of the Se^tBu groups as diagonally hatched spheres.

$$\left[Ag_{114}Se_{34}(Se^nBu)_{46}\left(P^tBu_3\right)_{14}\right]$$

$$\uparrow\ P^tBu_3$$

$$Ag(C_{11}H_{23}CO_2) + {}^nBuSeSiMe_3$$

$$\downarrow\ dppp$$

$$\left[Ag_{172}Se_{40}(Se^nBu)_{92}(dppp)_4\right]$$

SCHEME 3 Synthetic route to the Ag_{114} and the Ag_{172} clusters.

III. FROM BUILDING BLOCKS VIA CLUSTERS TO SOLIDS

The one-pot synthesis of ring-shaped and spherical polyoxometalates, based on a set of structurally conserved building blocks, has been another highly successful route to clusters of nanoscopic dimensions containing cavities and, in principle, pores. Such syntheses have been found to be based upon a building block principle with units that are suggested to have intrinsic properties (variable charge and flexible coordination modes) that facilitate the self-assembly of clusters containing many thousands of atoms in solution (Fig. 9). In this respect, the use of pentagonal-type building groups, with different symmetries, plays a key role in the formation of these systems as pentagonal units allow the construction of clusters with curvature that in turn prevents immediate growth to bulk materials.

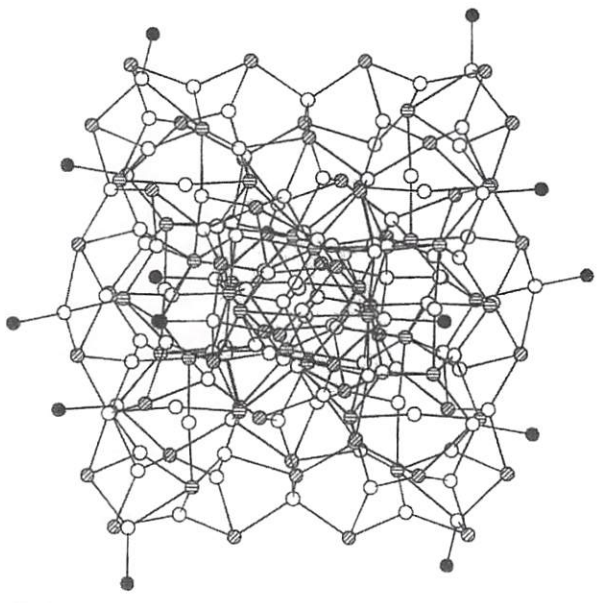

FIGURE 6 Molecular structure of $[Ag_{114}Se_{34}(Se^nBu)_{46}(P^tBu_3)_{14}]$. Ag atoms are shown as empty spheres, Se atoms depicted as horizontally hatched spheres, and the Se atoms of the Se^nBu groups as diagonally hatched spheres.

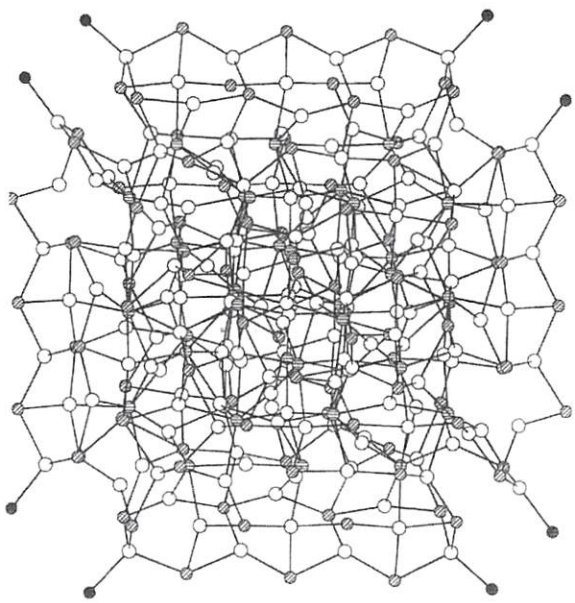

FIGURE 7 Molecular structure of $[Ag_{172}Se_{40}(Se^nBu)_{92}(dppp)_4]$. Ag atoms are shown as empty spheres and Se atoms depicted as horizontally hatched spheres, the Se atoms of the Se^nBu as diagonally hatched spheres, and the P atoms as black spheres.

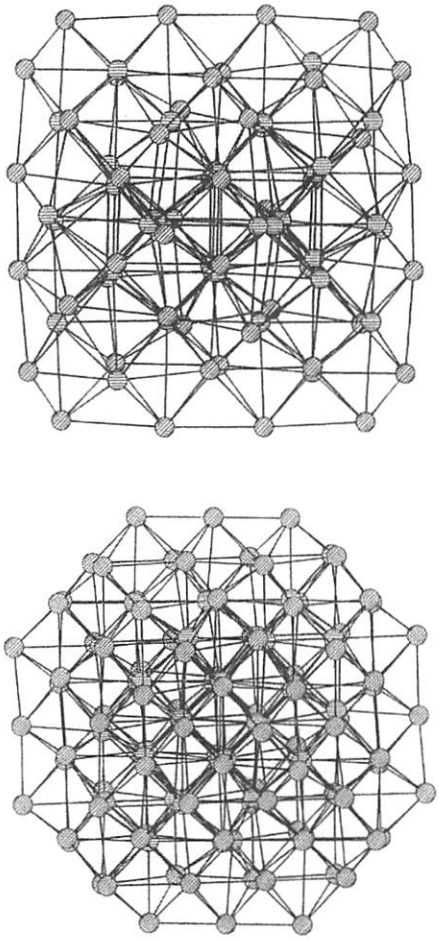

FIGURE 8 Se skeleton in $[Ag_{114}Se_{34}(Se^nBu)_{46}(P^tBu_3)_{14}]$ (above) and $[Ag_{172}Se_{40}(Se^nBu)_{92}(dppp)_4]$ (below). Se atoms are depicted by the horizontally hatched spheres and the Se atoms of the Se^nBu groups as diagonally hatched spheres.

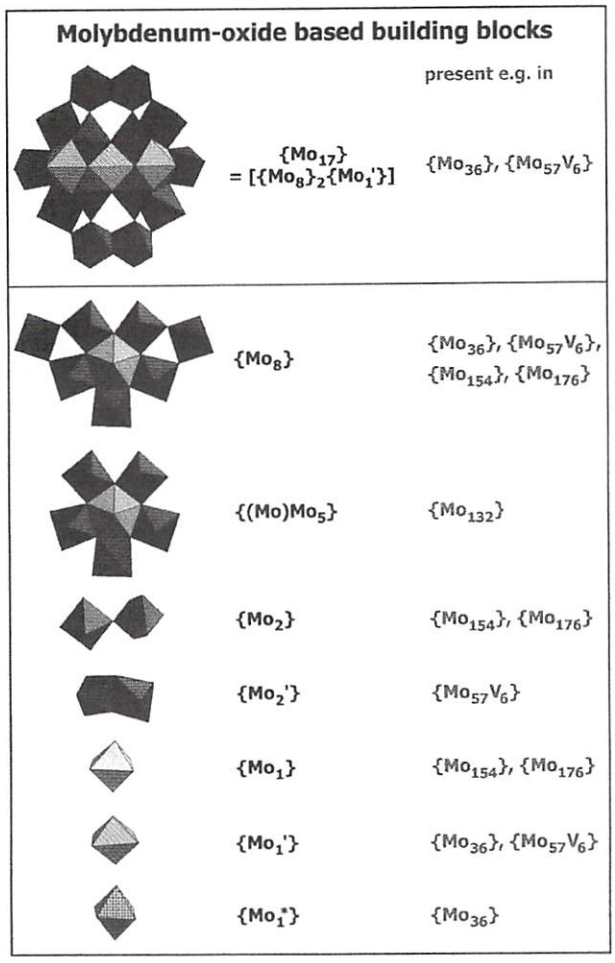

FIGURE 9 Molybdenum-oxide-based building blocks.

The most important strategy to promote growth of polyoxometalate clusters requires the generation of sufficiently negatively charged fragments/intermediates formed during the aggregation process. This can be attained not only by substituting some lower valence metal centers for ones of higher oxidation state or by substituting less positively charged for higher positively charged groups (e.g., by exchanging $[Mo(NO)]^{3+}$ for $[MoO]^{4+}$), but mainly by the presence of an appropriate reducing agent or even different types of these. The growth processes are promoted by the overall solubility of the growing cluster in solution-preventing aggregation, which can be achieved by avoiding nucleophilicity of the peripheral oxygen atoms that is too high. The presence of numerous H_2O ligands causes high solubility in protic media and terminal double-bonded oxygen atoms of the O=Mo groups prevent aggregation.

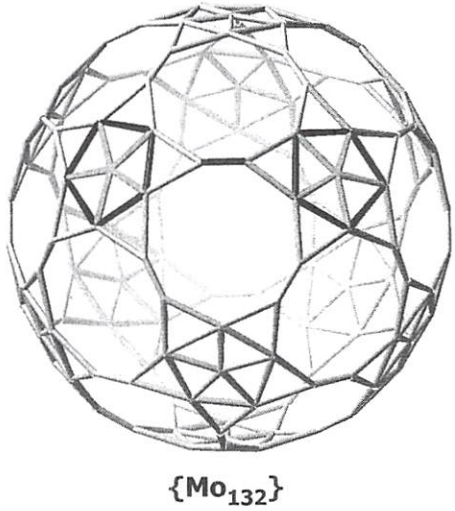

FIGURE 10 Schematic representation of the 132 molybdenum atom framework of the Keplerate cluster highlighting its spherical nature. Two pentagonal $\{(Mo)Mo_5\}$ groups linked by an $\{Mo^V\text{-}Mo^V\}$ bridge are emphasized.

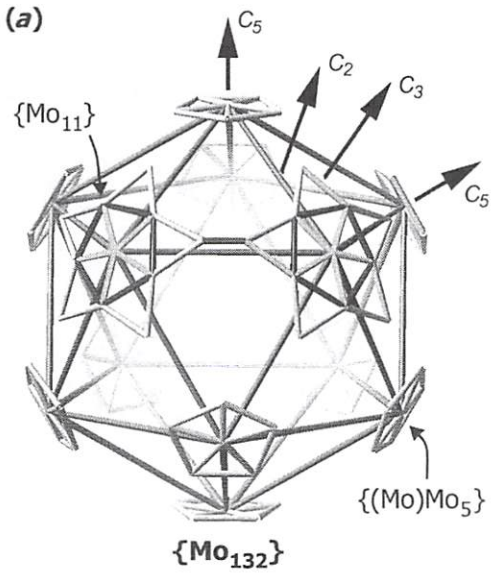

FIGURE 11 Schematic representation of the icosahedron spanned by the centers of the {(Mo)Mo_5} subfragments of the {Mo_{132}}-type cluster. Two of the {Mo_{11}} units each formed by the {(Mo)Mo_5} groups and the five related Mo centers of the five neighboring {$Mo^{V}{}_2O_4{}^{2+}$} bridges are emphasized.

A. Superfullerene Clusters with Icosahedral Symmetry

It is possible to construct a giant species similar in size and shape to spherical viruses with icosahedral symmetry (i.e., having C_5, C_3, and C_2 axes) from a reaction system in which pentagonal units with C_5 symmetry can first be generated, then get linked and placed at the 12 corners of an icosahedron. In the case of polyoxomolybdates, these pentagonal units of the type {(Mo)Mo_5} consist of a central pentagonal bipyramidal MoO_7 unit sharing edges with 5 MoO_6 octahedra. The {(Mo)Mo_5} unit is itself a constituent of the {Mo_8}-type unit abundant in many giant polyoxomolybdates (see below) in which two additional MoO_6 octahedra are bound (sharing corners) to the {(Mo)Mo_5} unit. In the presence of linkers, units which are capable of bridging two (or more) building blocks, for instance, those of the classical $[Mo^{V}{}_2O_4]^{2+}$ type (typically formed in reduced molybdate solutions in the presence of bidentate ligands), an icosahedral molecular system with 12 of the mentioned pentagons and 30 of the mentioned linkers is formed with the stoichiometry $[Mo^{VI}{}_{72}\,Mo^{V}{}_{60}O_{372}(CH_3COO)_{30}(H_2O)_{72}]^{42-}$ ({Mo_{132}}).

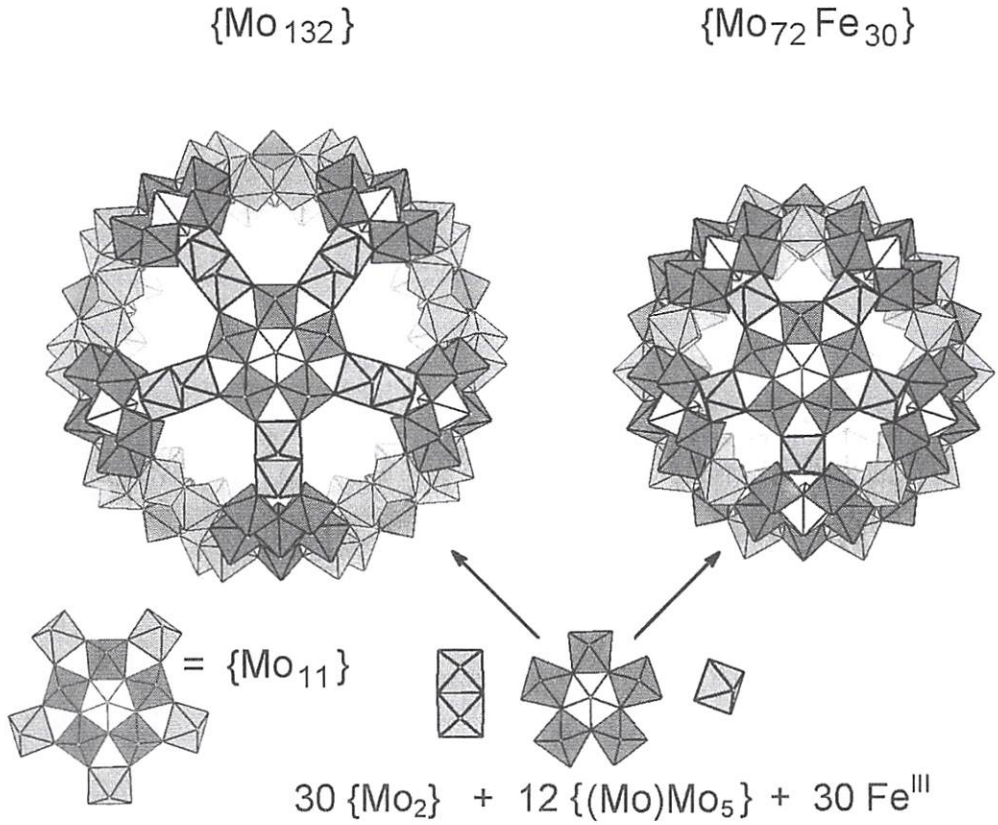

FIGURE 12 Comparison of the polyhedral representations of the {Mo_{132}} (left-hand side) and {$(Mo)^0(Mo_5)^I(Fe_{5/2})^{II}$}$_{12}$ (right-hand side) spherical clusters. The pentagonal centers of the {Mo(Mo_5)} are shown in white, the {Mo_2} groups and Fe-based octahedra are shown as light gray polyhedra, and the remaining (Mo_5) as dark gray polyhedra.

The central Mo positions of the 12 {(Mo)Mo_5} pentagons define an icosahedron and the 30 [$Mo^{V}{}_2O_4{}^{2+}$] a truncated icosahedron. This corresponds to the formulation [{(Mo)$Mo_5O_{21}(H_2O)_6$}$_{12}${$Mo^{V}{}_2O_4(CH_3COO)$}$_{30}$]$^{42-}$. The ball-like structure (Fig. 10) is also documented in the crystal structure (space group $Fm\bar{3}$) with cubic closest-packed spheres in the salt $(NH_4)_{42}[Mo^{VI}{}_{72}Mo^{V}{}_{60}O_{372}(CH_3COO)_{30}(H_2O)_{72}]$ • ca. 300 H_2O • ca. 10 CH_3COONH_4.

This molecular system with its 60 MoO_6 subunits, corresponding to the 12 related {(Mo)Mo_5} pentagons, represents a topological model for spherical viruses, e.g., the most simple satellite tobacco necrosis virus (STNV) with 60 identical protein subunits coded only by one gene. These form the 12 pentagonal capsomers (morphology units), each capsomer consists of five protomers.

Such spherical {Mo_{132}}-type clusters have been referred to in the literature as Keplerates corresponding to Kepler's model of the cosmos and his concept of planetary motion, as described in his early opus *Mysterium Cosmographicum*. In accordance with this speculative model, Kepler believed that the distances between the orbits of the planets could be explained if the ratios between the successive orbits were designed to be equivalent to the spheres successively circumscribed around and inscribed within the five Platonic solids.

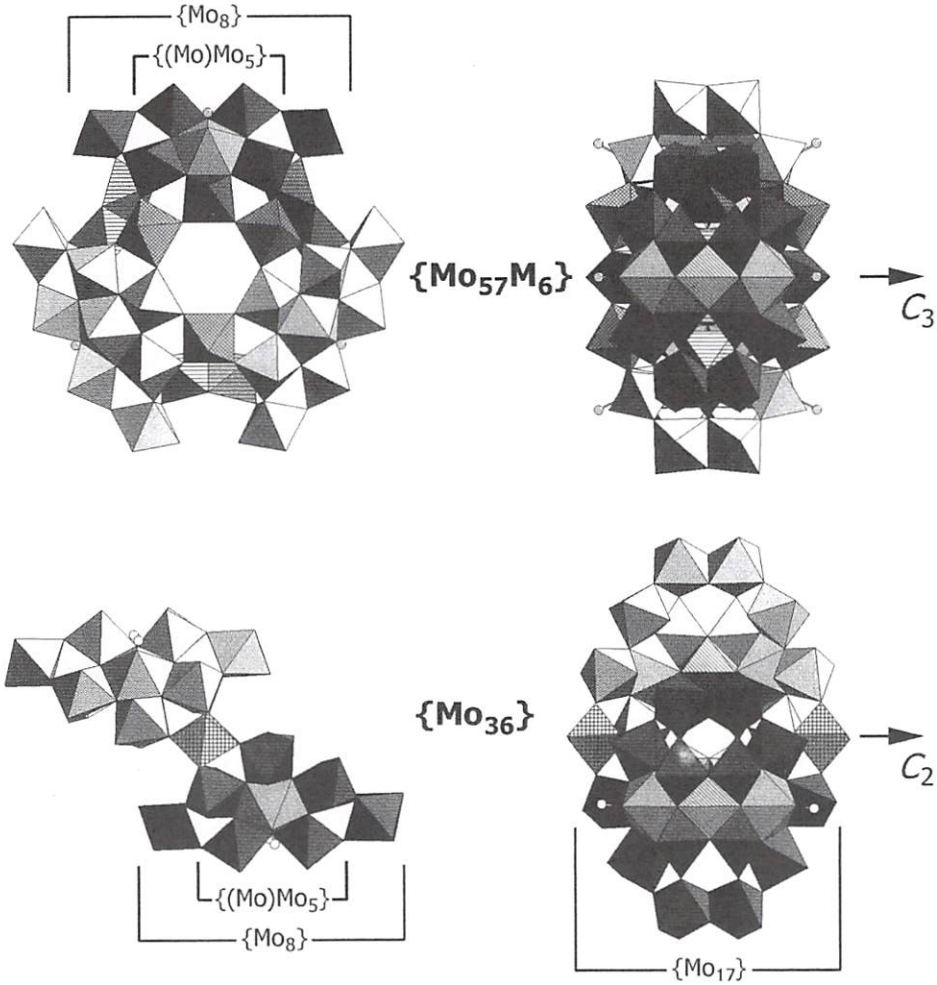

FIGURE 13 Polyhedral representation of the {$Mo_{57}M_6$} cluster with its basic building blocks and their constituents along the C_3 (upper left) and along one of the three C_2 axes (upper right). On the upper right, one {Mo_{17}} building block consisting of one {Mo_1'} and two {Mo_8} groups, and on the upper left, one {Mo_8} unit is shown by dark gray shading. Also shown by dark gray shading are one {Mo_2'} group (built up from two face-sharing octahedra) and one MO_6 unit (cross hatched). For comparison, the polyhedral representations of the {Mo_{36}} cluster structure, consisting of two {Mo_{17}} building blocks linked by two {Mo_1^*} units, are shown in the related views, also highlighting one {Mo_8} (bottom left) and one {Mo_{17}} building block (bottom right). It is important to recognize the relationship between the {Mo_8} and the pentagonal {(Mo)Mo_5} groups (see text). ({Mo_8}: light gray (central MoO_7 pentagonal bipyramid: white), {Mo_2'}: black, {Mo_1'}: hatched, {Mo_1^*}: cross hatched)

In analogy, the cluster correspondingly shows spherical shells of terminal oxygen and molybdenum atoms in which an icosahedron spanned by the centers of the 12 $\{(Mo)Mo_5\}$ pentagons—the Mo atoms of the central MoO_7 bipyramids—is inscribed (see Fig. 11). The $\{Mo_{132}\}$-type cluster has been the starting point for the development of a Keplerate-type chemistry illustrated by the fact that these types of species are stable in aqueous solution and allow the encapsulation of different types of guests into the cavity. It is possible to replace the $\{Mo_2^V\}$-type linker units by Fe^{III} ions which results in a $\{((Mo)Mo_5)_{12}Fe_{30}\}$-type cluster (a discrete cluster with the largest number of paramagnetic centers known). Such exchange reactions also allow resizing of the cluster shells while keeping the icosahedral symmetry (Fig. 12).

B. The Route to Wheel and Giant-Wheel Structures

In generating large complex molecular species the corresponding natural processes are effected by the (directed as well as nondirected) linking of (a huge variety of) basic and well-defined preorganized (or stepwise organized) fragments. An impressive example of this is the self-aggregation/reconstitution process of the tobacco mosaic virus (TMV) from preorganized units. This process more or less meets the strategy of controlling the linking of fragments to form larger units and linking the latter again. The linking of building blocks containing 17 metal atoms ($\{Mo_{17}\}$ units) to form cluster anions consisting of two or three of these units provides an archetypal example. The resulting 2- or 3-fragment clusters are of the $\{Mo_{36}\}$ $([\{MoO_2\}_2\{H_{12}Mo_{17}(NO)_2O_{58}(H_2O)_2\}_2]^{12-} = [\{Mo_1^*\}_2(\{Mo_8\}_2\{Mo_1'\})_2])$ or of the $\{Mo_{57}M_6\}$ type (e.g., $[\{VO(H_2O)\}_6\{Mo_2(\mu\text{-}H_2O)_2(\mu\text{-}OH)\}_3\{Mo_{17}(NO)_2O_{58}(H_2O)_2\}_3]^{21-} \equiv [\{VO(H_2O)\}_6\{Mo_2'\}_3(\{Mo_8\}_2\{Mo_1'\})_3]$) (Fig. 13).

The structure of the $\{Mo_{17}\}$ unit can be reduced to two $\{Mo_8\}$-type groups which are symmetrically linked by an $\{Mo_1'\}$-type unit. The $\{Mo_8\}$ building block, found in many other large polyoxometalate structures, is itself (as mentioned above) built up from a densely packed

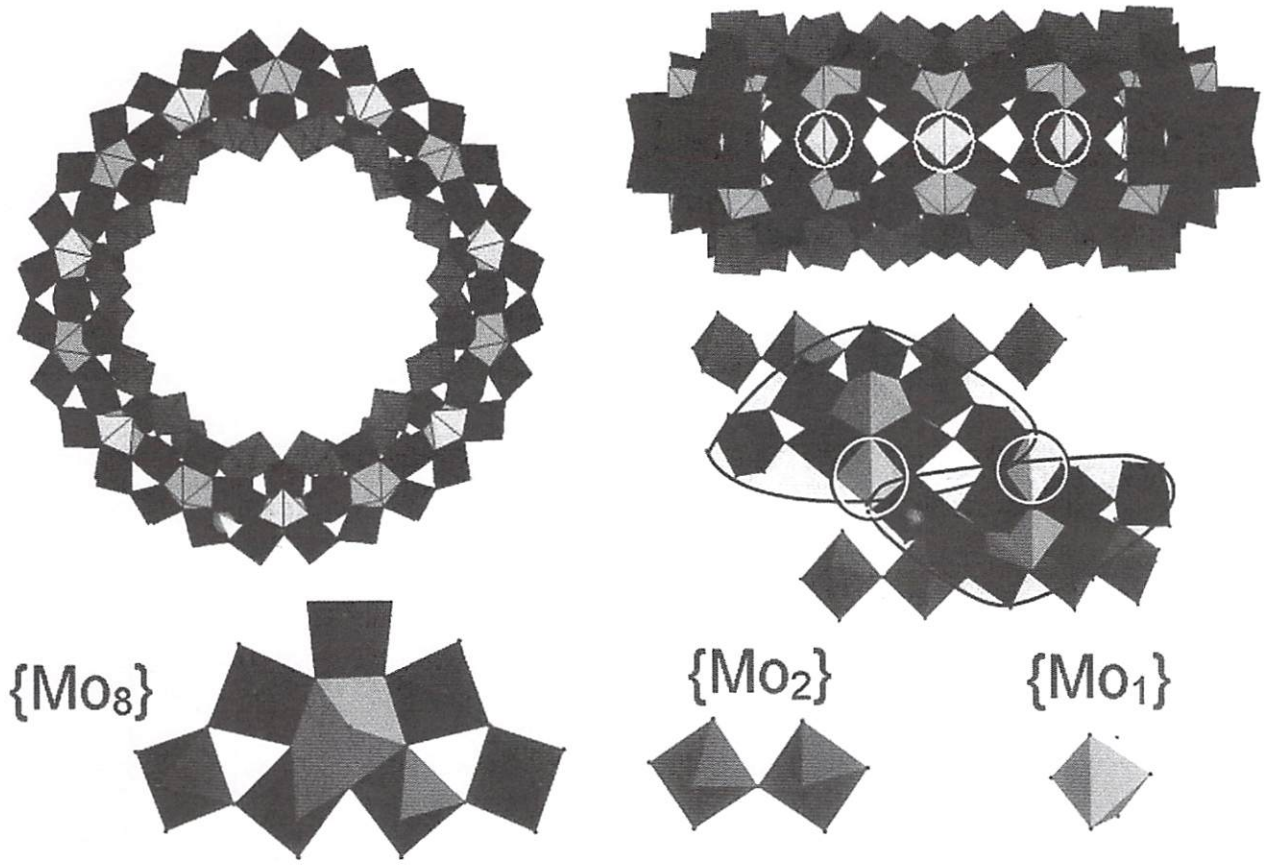

FIGURE 14 Schematic representation of the general architecture principle for the Giant-Wheel-type clusters, using the $\{Mo_{154}\}$ cluster (top view left-hand side and side view right-hand side) as an example. The structural building blocks for all Giant-Wheel clusters can be formulated as comprising $\{Mo_8\}$ units that are connected together via the $\{Mo_2\}$ units on the inner side of the wheel. Finally, the $\{Mo_1\}$ units form the equatorial plane of the ring linking the $\{Mo_8\}$ units together above and below the equator (the $\{Mo_1\}$ units are circled in the side view of the cluster for clarity).

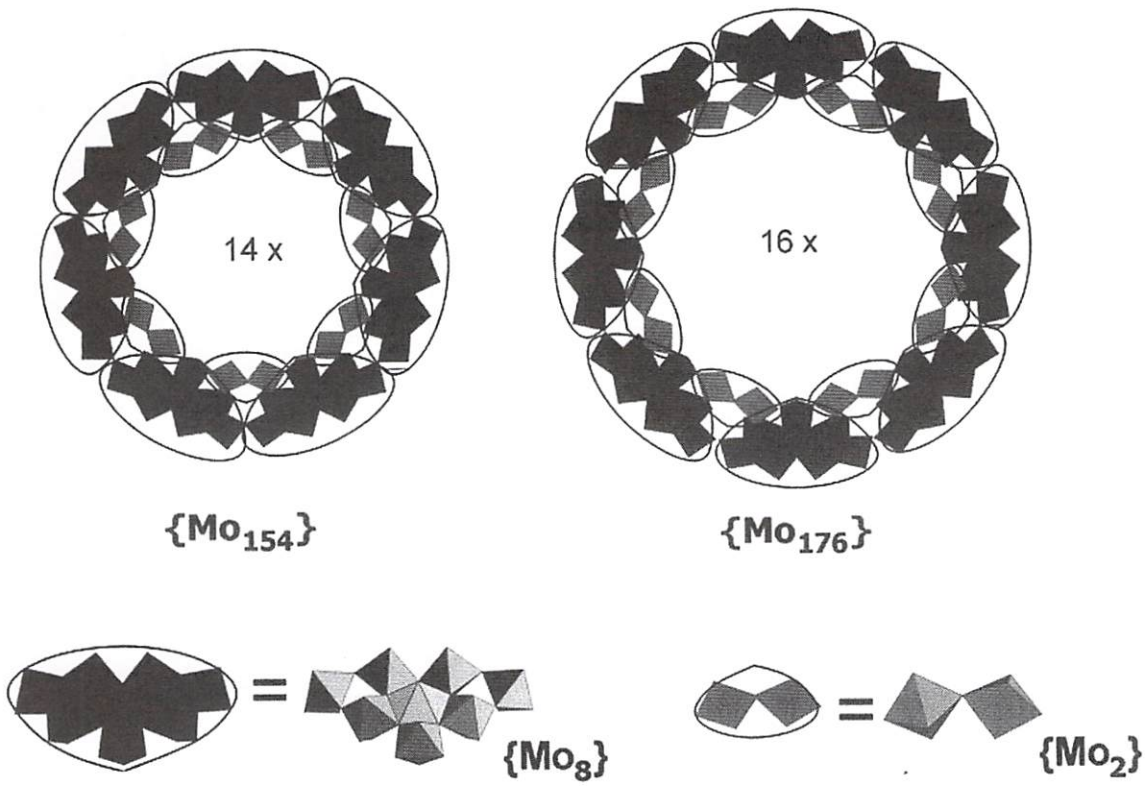

FIGURE 15 A representation of the upper halves of the tetradecameric $\{Mo_{154}\}$ and the hexadecameric $\{Mo_{176}\}$ Giant-Wheel clusters. The $\{Mo_8\}$ and $\{Mo_2\}$ building blocks are shown below. The equatorial $\{Mo_1\}$ building blocks, which connect the two sides of the Giant-Wheels together are not visible in this representation.

pentagonal $\{(Mo)Mo_5\}$ unit—containing a central MoO_7 or $MoO_6(NO)$ bipyramid sharing edges with five MoO_6 octahedra—with two more "weakly bound" (sharing only corners) MoO_6 octahedra which can be more easily removed. The pentagonal unit with a high formation tendency is, for instance, responsible for the formation of curved structures and, therefore, icosahedral symmetry like the $\{Mo_{132}\}$-type cluster (see Fig. 11).

With $\{Mo_8\}$-, $\{Mo_2\}$-, and $\{Mo_1\}$-type building blocks (Fig. 9) even larger and unusual clusters can be built up, for example, the 3.5-nm-diameter, wheel-shaped metal-oxide-based cluster anion containing 154 molybdenum atoms $[(MoO_3)_{154}(H_2O)_{70}H_{14}]^{14-} \equiv [\{Mo_2\}_{14}\{Mo_8\}_{14}\{Mo_1\}_{14}]^{14-}$ ($\{Mo_{154}\}$). The cluster above contains 14 of the mentioned $\{Mo_8\}$ groups linked by 14 $\{Mo_2\}$- and 14 $\{Mo_1\}$-type units, respectively (Figs. 14 and 15).

Overall, the complete ring system consists formally of 140 MoO_6 octahedra and 14 pentagonal bipyramids of the type MoO_7, see Fig. 14. The basic building blocks of the tetradecameric wheel are $14\{Mo_8\}$ units with a central MoO_7 group. This MoO_7 group is symmetrically connected to five MoO_6 octahedra by edge sharing resulting in

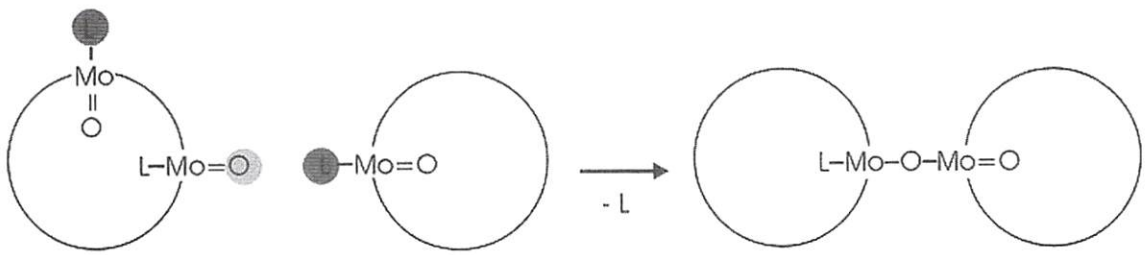

FIGURE 16 Schematic representation of the basic assembly principle of the Giant-Wheel-shaped cluster units forming the networks and layers. The formation is based on the synergetically induced functional complementarity of the $\{Mo_2\}$ units O=Mo(L) (L=H_2O, $H_2PO_4^{2-}$).

an {(Mo)Mo_5} pentagon. Four of the MoO_6 octahedra are linked to two MoO_6 octahedra via corners to form the basic {Mo_8} unit. Continuing from the {Mo_8} unit the complete {Mo_{154}} cluster ring is built up as follows: (1) those two MoO_6 octahedra which are not directly connected to the central MoO_7 bipyramid are fused to neighboring {Mo_8} units through corners; (2) neighboring {Mo_8} groups are additionally fused together by the {Mo_2} units, thereby completing the inner-ring parts of the upper and lower half of the ring structure; and (3) the complete ring is constructed when the second half is rotated around 360/14 degrees relative to the first and fused to it through the 14 {Mo_1} groups, which are located at the equator of the complete ring, see Fig. 14.

The synthesis of the tetradecameric {Mo_{154}} cluster type can be related to that of the hexadecameric {Mo_{176}} cluster. The most important change is that this requires reaction conditions with a pH lower than in the smaller ring system and the presence of an increased concentration of molybdate. The {Mo_{176}}≡[{Mo_2}$_{16}${Mo_8}$_{16}${Mo_1}$_{16}$]$^{16-}$ cluster with the formula [$(MoO_3)_{176}(H_2O)_{80}H_{16}$]$^{16-}$ comprises two extra {Mo_8}, {Mo_2}, and {Mo_1} units, respectively, when compared to the smaller {Mo_{154}} cluster, see Fig. 15.

C. Introduction of Defects and Linking the "Giant-Wheel" Clusters to Chain and Layer Networks

It is possible to obtain Giant-Wheel-type clusters that are structurally incomplete, i.e., comprising defects when compared to the original {Mo_{154}} cluster. Such defects manifest themselves as missing {Mo_2} units. (These defects can sometimes be seen as underoccupied {Mo_2} units when the distribution suffers from rotational or translational disorder within the crystal structure.) It should be noted, however, that as the introduction of defects increases the overall negative charge, the rings can be linked together into chains and layers. In general, this type of linking reaction occurs via the terminal {Mo_2}-based H_2O—Mo=O groups (see Fig. 16). For example, an

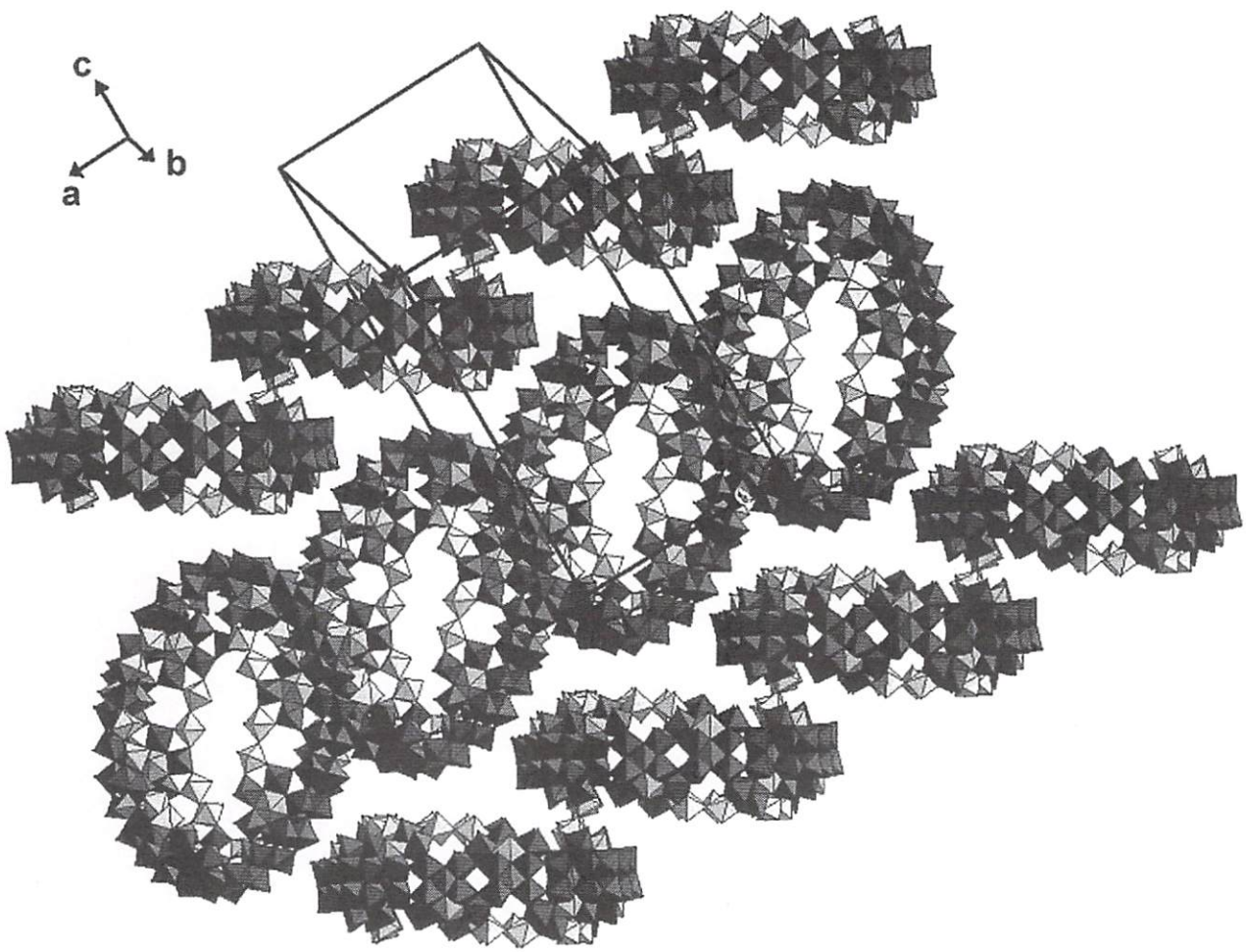

FIGURE 17 Polyhedral representation of {Mo_{144}} units linked to chains. Linking occurs via the {Mo_2} units.

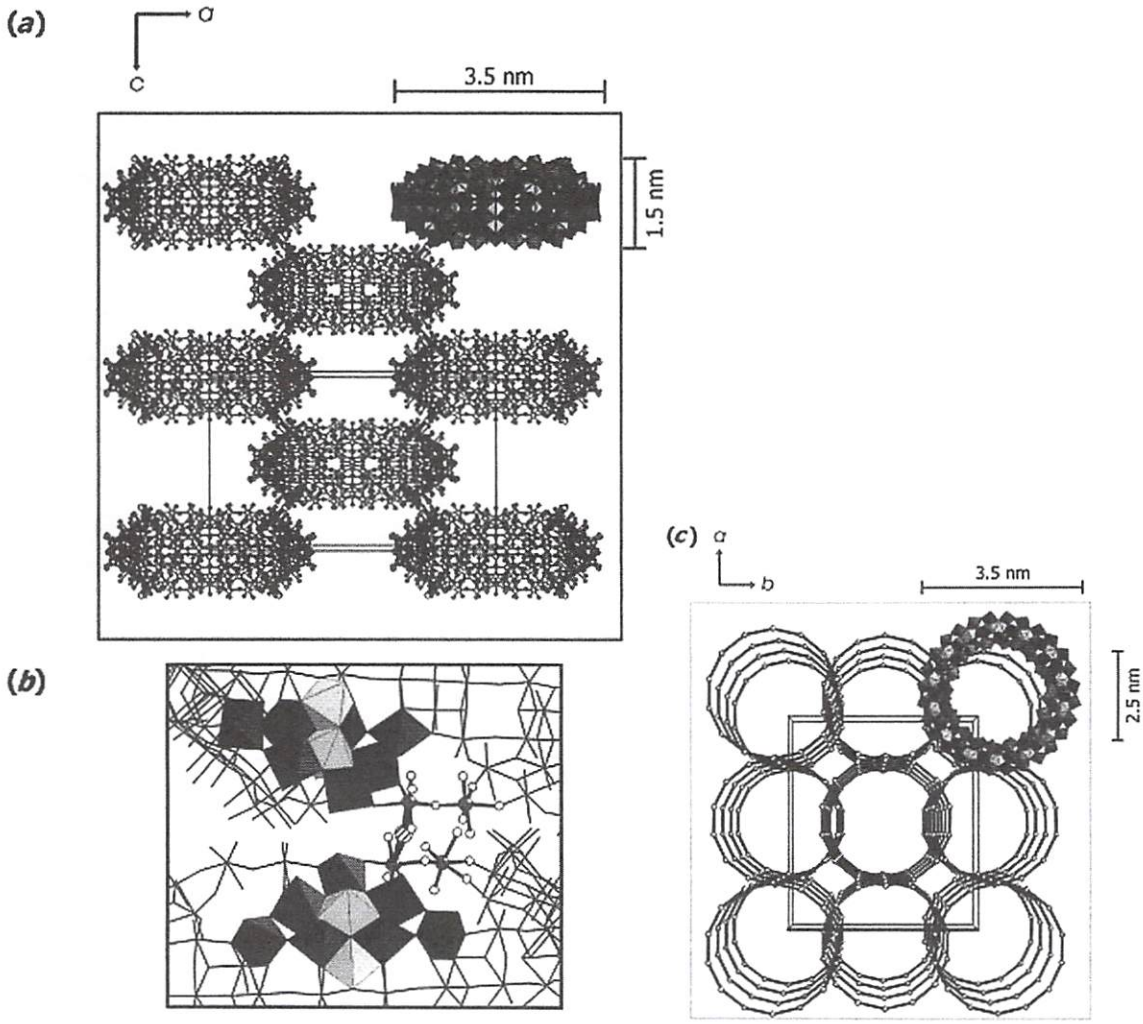

FIGURE 18 Ball and stick representation of the "packing" of the linked rings (in the direction of the *b* axis) in crystals of $Na_{16}[Mo^{VI}_{124}Mo^{V}_{28}O_{429}(\mu_3\text{-}O)_{28}H_{14}(H_2O)_{66.5}]$. XH_2O ($X \approx 300$) ($\{Mo_{152}\}$) viewed along the crystallographic *b* axis. (a) Each ring is connected to surrounding rings via Mo-O-Mo bridges of the O=Mo-O-Mo-OH_2 units, thus forming layer networks parallel to the *ac* plane. One ring is shown as basic unit in polyhedral representation. (b) Detailed view of the bridging region between two cluster rings. One $\{Mo_8\}$ unit of each ring along with one $\{Mo_1\}$ unit is shown in polyhedral representation and one $\{Mo_2\}^{2+}$ ($=\{Mo^{VI}_2O_5(H_2O)_2\}^{2+}$) unit per ring in ball and stick representation. (c) Perspective view along the crystallographic *c* axis showing the framework with nanotubes that are filled with H_2O molecules and sodium cations. For clarity, only one ring is shown in a polyhedral representation. For the other rings only the equatorial $\{Mo_1\}$ units are given and connected.

$\{Mo_{144}\}$ defect cluster can be linked to chains (see Fig. 17) and an $\{Mo_{152}\}$ cluster can be linked in the construction of a layered compound (see Fig. 18).

D. Nucleation Processes within a Cluster Cavity—from an $\{Mo_{176}\}$ to an $\{Mo_{248}\}$ Cluster

Under special types of reducing conditions (using ascorbic acid as a reducing agent) the $\{Mo_{176}\}$ cluster can be observed to grow; during this process a further two $\{Mo_{36}\}$ units are "added" to each side of the cluster forming a spherical disk-shaped cluster comprising 248 Mo atoms. The hubcaps were found in the mixed-crystal compound to have an occupation of 50%, see Fig. 19. This appears to be a remarkable result when it is considered that the larger wheel cluster "cap," the $[Mo_{36}O_{96}(H_2O)_{24}]$-type fragment, is nearly identical to a segment of the solid-state structure of the compound Mo_5O_{14} (see Fig. 20). This extraordinary structure (the largest discrete inorganic structure to be characterized by single crystal X-ray diffraction to date) offers the possibility of model crystal growth

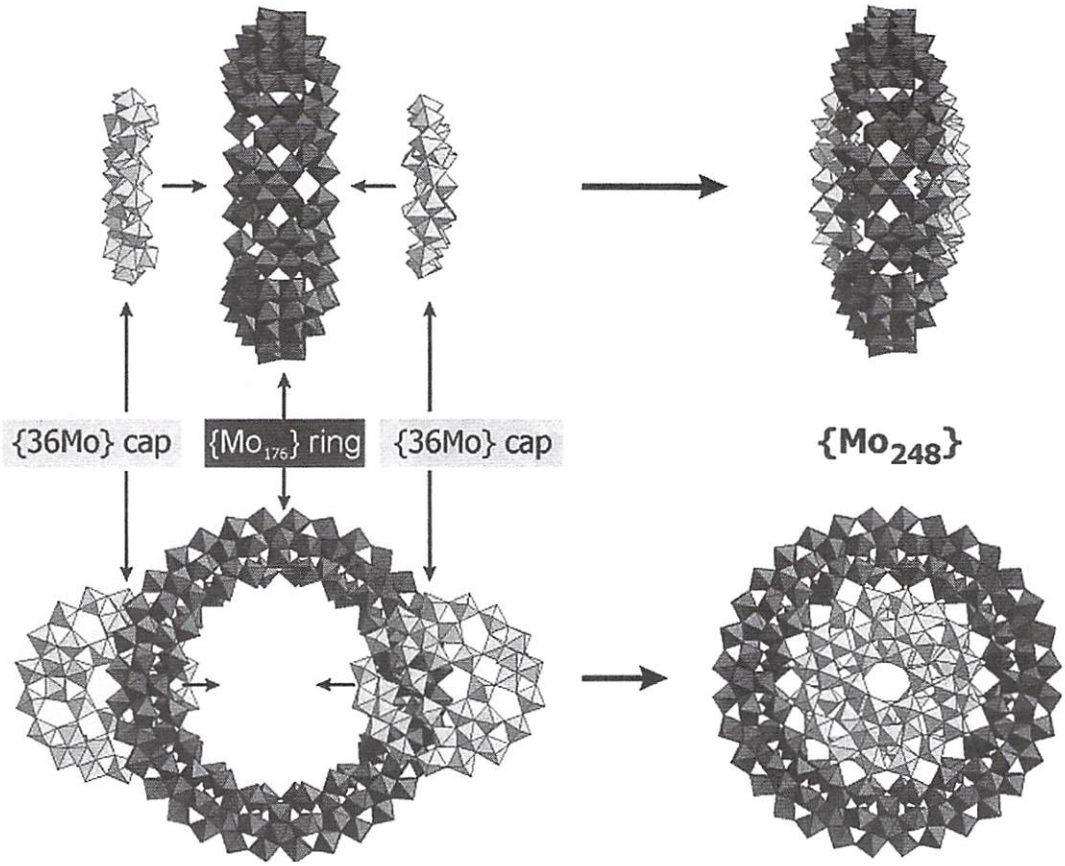

FIGURE 19 Schematic representation of the growth process $\{Mo_{176}\} \rightarrow \{Mo_{248}\}$. The structure of one $\{Mo_{248}\}$ cluster can formally be decomposed into one $\{Mo_{176}\}$ ring and two $\{Mo_{36}O_{96}(H_2O)_{24}\}$ "hubcaps."

under boundary conditions, especially the related nucleation process. Of particular note is that the growth event can be considered to start from the inner $\{Mo_2\}$ groups, see Fig. 19.

IV. CONCLUSIONS AND PERSPECTIVES

It seems to be worthwhile to try to correlate aspects of nanostructured giant discrete clusters and related solid-state structures, which is possible for molybdenum-oxide, metal-chalcogenide, and pure metal-based systems. On investigating the border region between the molecular and the macroscopic world, several questions arise, for instance, whether the size of such cluster systems has a limit or whether we can fabricate ever larger assemblages approaching (the limit of) the macroscopic world. The synthesis of gold, palladium, and related clusters protected with ligands or as colloidal dispersions may provide a direct route to new materials with novel electronic properties. From another point of view, the nanosized polyoxomolybdate clusters provide model objects for studies on the initial nucleation steps of crystallization processes, an interesting aspect for solid-state chemists and physicists as the initial steps for crystal growth are not known. It is remarkable that using the same reaction type, i.e., the acidification of aqueous solutions of the most simple tetrahedral oxoanions of the early transition elements of the type MO_4^{n-}, the (resulting) products span the three important areas of matter, from the micro-, through the meso- (or nano-), to the macrostructures, the latter being characterized by periodicity or translational invariance. The use of the above-mentioned fundamental linkable building units, e.g., in the form of Platonic solids such as tetrahedra or octahedra, enables the generation of molecular systems of higher structural variability and versatility compared to arrangements of aggregated metal atoms with spherical symmetry. It appears that through the synthesis of inorganic clusters man is developing a level of control from the molecular through the nanoscale to bulk material that will allow the construction of materials having a massive impact both in our understanding of conservative self-organization processes and the development of materials of interest for technology.

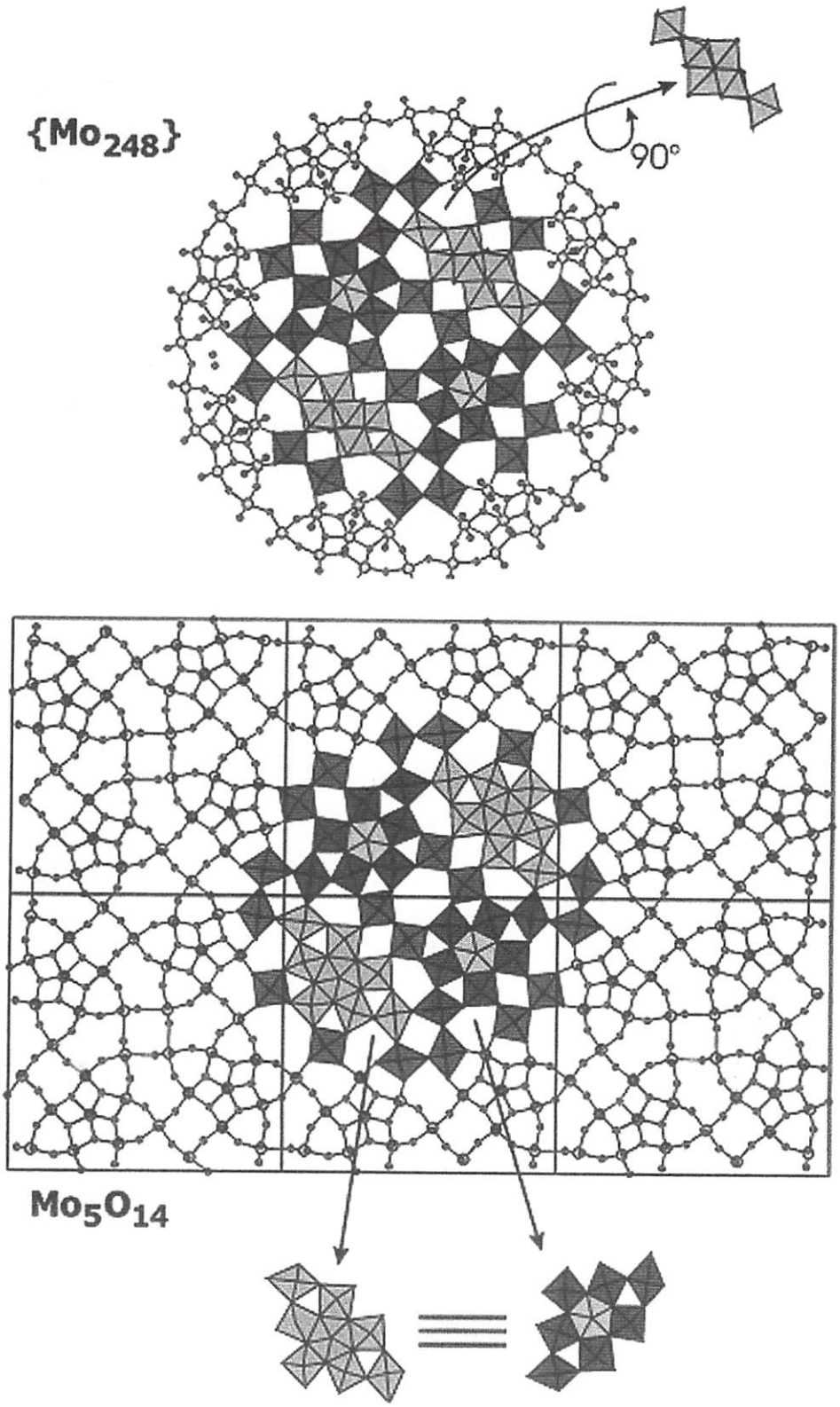

FIGURE 20 Structural comparison of the hubcap motif of the $\{Mo_{248}\}$ cluster (above) and the related segment of the solid-state structure $\{Mo_5O_{14}\}$ (below).

SEE ALSO THE FOLLOWING ARTICLES

METAL CLUSTER CHEMISTRY • METAL PARTICLES AND CLUSTER COMPOUNDS • SOLID-STATE CHEMISTRY

BIBLIOGRAPHY

Cronin, L., Kögerler, P., and Müller, A. (2000). *J. Solid State Chem.* **152,** 57.

Kozitsyna, N. Y., and Moiseev, I. I. (1995). *Russ. Chem. Rev.* **84,** 47.

Müller, A., Fenske, D., and Kögerler, P. (1999). *Curr. Op. Solid State Mater. Chem.* **4,** 141.

Müller, A., Kögerler, P., and Bögge, H. (2000). *Struct Bonding* **96,** 203.

Müller, A., Kögerler, P., and Kuhlmann, C. (1999). *Chem. Commun.* 1347.

Schmid, G. (1996). In "From Simplicity to Complexity in Chemistry—and Beyond," (A. Müller, A. Dress, and F. Vögtle Part I, eds.), Vieweg Braunschweig, Wiesbaden, Germany.